Synthesis and Validation of Wideband Excitation Coefficients in Plane Wave Generator Systems

F. Saccardi[1], A. Giacomini[1], V. Schirosi[1], L.J. Foged[1], N. Gross[2], S. Anwar[2], E. Kaverine[2], E. Szpindor[3], T. McKeown[3]

[1] MVG Italy, Via Castelli Romani, 59, Pomezia, Italy, lars.foged@mvg-world.com

[2] MVG Industries, 13 Rue du Zéphyr, 91140 Villejust, France, nicolas.gross@mvg-world

[3] MVG Orbit Advanced Technologies Inc., 650 Louis Drive, Warminster, PA, US

***Abstract*—Plane Wave Generators (PWG) are arrays of elements arranged and excited to approximate a plane wave, creating far-field conditions within a Quiet Zone (QZ) in the near-field proximity of the array. Thanks to its compact design, the PWG offers a closer approximation to far-field conditions compared to equivalently sized Compact Antenna Test Range (CATR) systems. However, the discrete sampling by the array elements of the PWG's radiating aperture constitutes a limit to the obtainable electrical size of the QZ. As a result, PWGs are commonly used in lower-frequency measurement applications, such as UHF and VHF, where system size is a key design constraint. Consequently, PWGs often serve as a viable alternative or, more commonly, a complement to traditional CATR-based solutions, particularly for lower-frequency testing. Although PWGs have attracted significant attention in the literature, including for wideband testing, the array excitation, specifically, the selection of complex weights for the radiating elements, has typically been addressed at discrete frequencies, assuming unique excitations for each frequency. In this paper, we focus on the synthesis of excitation coefficients valid across a decade bandwidth, enabling the system to support wideband signal testing, such as when modulated signals or time-domain gating and filtering are employed. The wideband coefficients are experimentally validated on a low-frequency PWG array, demonstrating the system's capability for effective wideband measurements.**

***Index Terms*—antenna meausrements, measurements, compact antenna test range, plane wave generators.**

I. INTRODUCTION

The Plane Wave Generator (PWG) concept has proven to be an effective approach for testing low-frequency antennas in compact anechoic environments [1], [2]. The optimum sizing of the PWG and the optimization of the excitation coefficients has attracted considerable interest in the literature [3]-[8]. Significant progress has been made recently in evolving the PWG concept into an industrial-grade testing solution for antennas, particularly for active device testing.

A dual-polarized PWG covering the 0.6–6 GHz frequency range was validated and reported in [9]. This compact design utilized 40 dual polarized elements on a circular aperture of 1.3λ_0, where λ_0 denotes the wavelength at the lowest operating frequency f_0. The QZ amplitude and phase variations was within ±1.0 dB and ±10.0° on an 8:1 bandwidth respectively, over a λ_0 diameter at 1.5λ_0 distance from the PWG aperture.

In [4], a design with 256 elements on a square aperture of 11.3λ_0, operating in the 2–5 GHz band, was presented and validated. The design achieved a QZ of 6λ_0 diameter at 14λ_0 distance from the PWG aperture with amplitude and phase variations of ±1.25 dB and ±7.5°.

In [10], a PWG consisting of 156, linear polarized elements on a square aperture of 10λ_0, was developed in the 1.7-5GHz frequency range with a QZ diameter size of 6λ_0 diameter at 9λ_0 distance from the PWG aperture with amplitude and phase variations of ±0.6 dB and ±5° at selected frequencies.

An elegant PWG based solution at millimeter frequencies has been presented [11] consisting of 172 dual polarized elements covering the 24-32GHz frequency band. The QZ diameter is 28λ_0 at 96λ_0 distance. This concept is particularly interesting as the antenna under test (AUT) is practically stationary with only a mechanical rotation in azimuth.

The PWG concept is particularly interesting for testing lower frequency, down to VHF/UHF range. In [12], this concept was successfully applied to test a 50-70 MHz antenna mounted on a CubeSat within an anechoic chamber designed for much higher frequencies. The PWG was composed of an array of virtual elements repositioned throughout the chamber, while the CubeSat was measured in two positions, shifted by $\lambda/4$. This configuration allowed for the mitigation of backwall radiation effects through post-processing. In [13] the concept was further refined into a versatile PWG system designed for the VHF/UHF frequency range, targeting a 10:1 frequency bandwidth. The array consists of approximately 100 miniaturized, dual-polarized radiating elements embedded in absorbing material, with an element spacing of 0.4λ_0. These elements are arranged over a surface with a diameter of approximately 4.5λ_0 between the furthest elements.

Common for the above-mentioned PWG solutions, the array excitation, i.e. the complex weights for the radiating elements, has traditionally been handled at individual frequencies, with a distinct array excitation applied for each frequency.

This paper focuses on the development and validation of excitation coefficients suitable for bandwidths spanning a decade or more, enabling the PWG system to support wideband signal testing, including scenarios with modulated signals or time-domain gating and filtering. This capability is achieved in PWG systems through the use of amplitude and phase shifters that operate over a broad frequency range [9], [14].

II. Proposed PWG solution for measurements at VHF and UHF frequencies

The proposed baseline dual polarized PWG array, designed for measurements at VHF/UHF frequencies over a 10:1 bandwidth is shown in Fig. 1. Its design is inspired by the CubeSat measurements at 50-70 MHz discussed in [12]. The array configuration is easily scalable to different frequencies within the VHF and UHF bands and can be adjusted by adding or removing radiating elements from the baseline 85-element setup to accommodate different quiet zone (QZ) sizes. The baseline array spans $6\lambda_0$ between the outermost elements and supports a QZ with a diameter of up to $4\lambda_0$, where λ_0 represents the wavelength at the lowest operating frequency. The QZ can be positioned at variable distances between $6\lambda_0$ and $20\lambda_0$ from the aperture, depending on the excitation. Each dual-polarized array element is embedded in absorbing material, with an inter-element spacing of $0.67\lambda_0$. The radiating elements are specifically engineered for PWG applications.

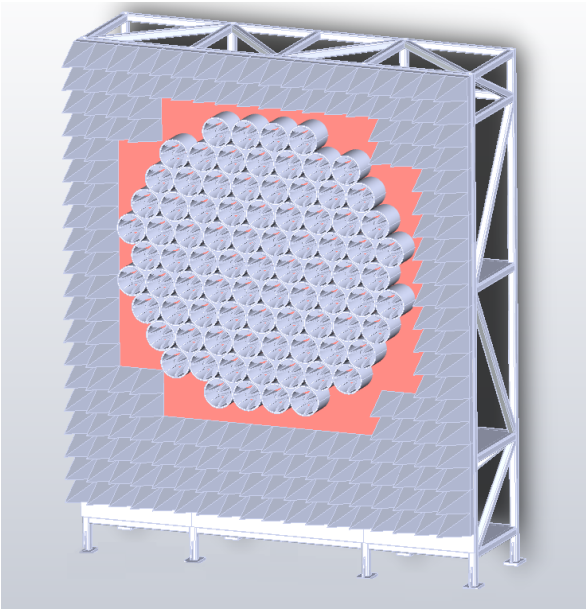

Fig. 1. Proposed PWG solution for measurements of wide band antennas and active decives at VHF/UHF frequencies.

The elements are arranged on a hexagonal grid, which is not optimal from an aperture sampling perspective, as theory suggests that element density can be reduced towards the edges of the radiating aperture [5]. However, the regular grid simplifies manufacturing, and the difference in number of elements is negligible for most applications. Additionally, the inter-element coupling, which can be significant at the lowest frequencies despite specific element designs and the use of absorbers, remains consistent across all internal elements. This uniformity enhances the design's robustness against coupling-induced errors.

Moreover, the number of elements, spacing, placement, QZ diameter, and distance can be adjusted based on the specific operational bandwidth and desired QZ ripple performance.

III. PWG Beam Forming Network

The Beam Forming Network (BFN) is a critical component of the system, responsible for distributing complex weights to each array element. The elements are organized into subarrays, each assigned identical amplitude and phase coefficients, distributed through a uniform network. To ensure phase matching between elements and support wideband frequency operation, all cables are of equal length. The amplitude and phase coefficients are controlled by analog components within the wideband amplitude/phase module, which is digitally managed as described in [9]. Amplitude variation is achieved using programmable attenuators, while phase variation is typically controlled by programmable phase shifters. Amplitude weights are controlled in 0.5dB steps on a 0-40dB dynamic range and phase are controlled in 2° steps. A typical layout of a BFN and a programmable amplitude-phase shifter are illustrated in Fig. 2.

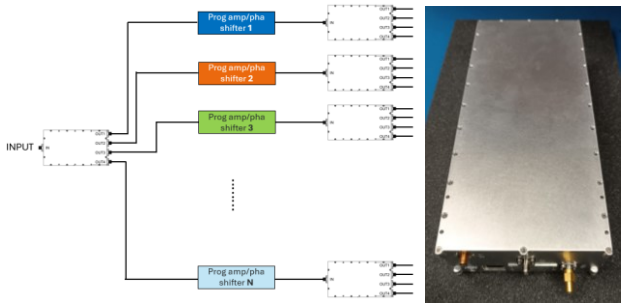

Fig. 2. Example of the PWG distribution network. The wideband BFN ensures phase matched, uniform amplitude and phase distribution across subarrays (left). Complex weights on subarrays are controlled by the wideband programmable amplitude and phase shifter developed for this validation (right).

This feeding approach eliminates the need for analog-to-digital or digital-to-analog conversions, preventing distortion in wideband signals, and is fully reciprocal, as it incorporates only linear components. While distributed amplification of the signals is not implemented in this design, it remains an optional capability. Fig. 3. shows the measured phase response of four different phase shifter modules. The imposed phase, ranging from 0° to 360°, remains stable across the entire 10:1 bandwidth, exhibiting minimal frequency dependence. This stability makes the modules ideal for wideband coefficient applications.

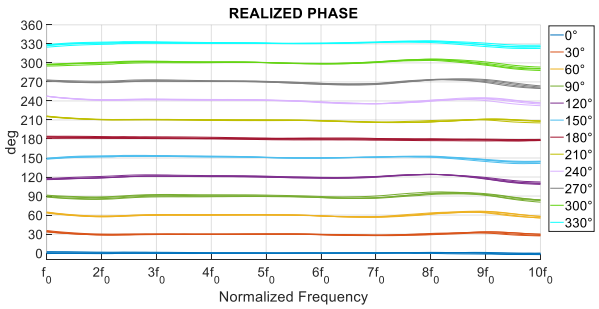

Fig. 3. Measured phase response of 4 different phase shifter modules in a 10:1 bandwidth.

IV. PWG Synthesis Strategy

The array excitation is defined through numerical optimization of a functional imposing the far field condition in the desired QZ. A set of discrete points, known as synthesis stations, often located on different planes, defines the QZ in the volume in front of the PWG. This is shown as planes of varying distance in Fig. 4 which is a convenient way to represent the QZ, as the same phase is needed on each plane. To represent the QZ correctly, several planes, usually 3 or more are needed.

To complete the optimization, the radiated field from every array element must be determined on each station. This field can be determined either through modelling using a representative numerical model of the array elements, array measurements in a test facility or in-situ measurement in the facility where the PWG is installed.

The goal of numerical optimization is to find the optimal weights for the array elements, subject to the constraints of the BFN, that minimize a defined objective function. A commonly used objective function is the maximum deviation in amplitude and phase between the synthesized field at the stations defining the QZ and the desired field. However, as noted in [5], this approach is suboptimal because it does not impose limits on the fields outside the QZ, particularly on the walls of the anechoic chamber where the PWG will be operating. Another drawback is that this method requires fixed target field levels within the QZ, which must be predefined, and this is not easy to know apriori to the optimization.

An alternative objective function that operates without fixed target field levels is presented in [15]. This method has been implemented for PWG optimization in [9] and is also applied in this work. In this approach, array coefficients are left unnormalized, with a constraint to maximize the total energy within the QZ. This formulation is advantageous because it minimizes the fields outside the QZ without requiring an additional constraint outside the QZ in the form of other stations. Furthermore, this method converts the optimization into a well-behaved real non-linear min-max problem, enabling classical optimization algorithms to determine the optimal array coefficients, even under the constraints of the BFN.

The optimization procedure is illustrated in Fig. 4. The numerical problem involves optimizing the composite power field $E_j = e_j e_j^*$ so that the amplitude and phase differences on all j stations are minimum to support the approximation to a plane wave. Two scaling constants A for amplitude and B for phase are introduced to scale the optimization problem effectively. By using non-normalized excitation coefficients α the optimization avoids setting absolute targets for amplitude and phase. Adjusting α, allows the amplitude E_j can be scaled to A and minimize the variation. The same can be done by varying the absolute phase of α to make it fit with the constant B. in the equation, c is a scaling constant matching amplitude and phase constraints.

When dealing with multi-frequency optimization, the target field level is flexible, but the differences between the levels at different frequencies need to the addressed in an intelligent way. This can be done by imposing a proper scaling between the target levels of each frequency. This scaling is included in the constant A that takes a different value for each frequency. Constant A can be fixed for the first frequency and the succeeding A values for other frequencies can be found as a product of the optimization itself.

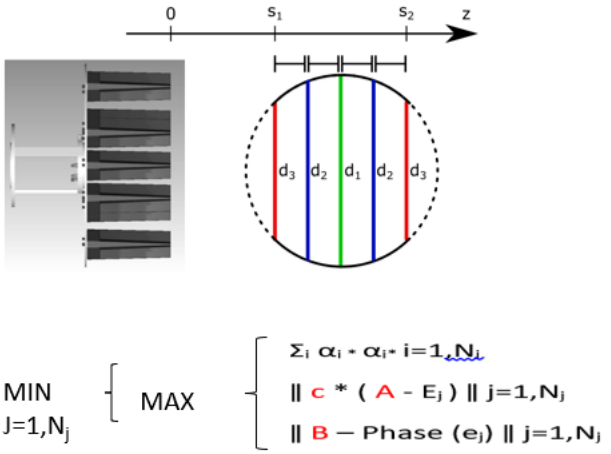

Fig. 4. Synthesis strategy for exitation coefficient optimisation over a wide bandwidth.

V. Validation Scenario and Discussion of the Measured Performance

A representative prototype sub-array, consisting of the 19 central elements of the proposed VHF/UHF frequency design, was manufactured and measured to validate the PWG design. The diameter of the considered sub-array is roughly 2.1λ₀, with an element spacing of 0.4λ₀. Different QZ syntheses were performed across the entire frequency range from f_0 to $10f_0$ to optimize specific sub-bands. Various QZ sizes and distances were also considered. It was observed that increasing the distance between the QZ and the array improved QZ performance during the wideband optimization of the coefficients, and it also enabled the creation of a larger QZ.

In this paper, the measurement results related to the following PWG configuration are reported:

- QZ diameter: $1\lambda_0$
- PWG to QZ distance: $3\lambda_0$
- Optimized sub-band: f_0 to $2f_0$

The validation measurements were performed in a MVG multi-probe spherical near-field automotive test range, operating from 70 MHz to 6 GHz, installed in the Pulsaart by AGC facility in Belgium [16]. The sub-array was positioned on the ground, radiating upwards into the hemispherical near-field (NF) system as shown in Fig. 5. As part of the validation, the measurements were compared to the full-wave digital twin model of the entire array. The digital twin was also used to generate the array excitation coefficients, which were applied in the BFN. Measurements of have been conducted on the extended 8:1 bandwidth from $0.5f_0$ to $4f_0$, to validate the digital twin predictions.

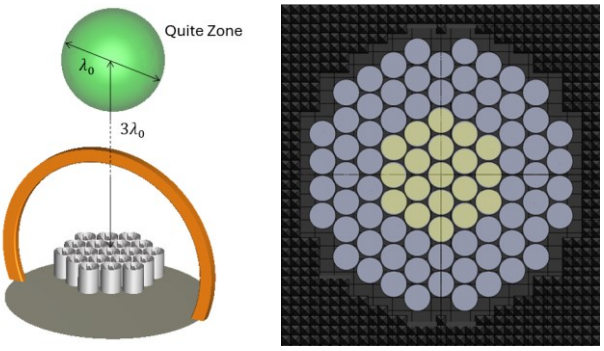

Fig. 5. Skecth showing the measurement scenario of the 19 element PWG array during validation measuremnt in the Pulsart by AGC spherical near field automotive range (left). Skecth showing the 19 element portion of the full 85 element PWG array designed at VHF/UHF frequencies.

Using the PWG array excitation coefficients from the optimization of the digital twin as inputs for the amplitude and phase settings of the BFN, Spherical NF (SNF) data radiated by the array, when driven through the BFN from a single port, was collected at the measurement distance and then propagated to the desired QZ distance using NF-to-NF post-processing. This technique is discussed further in [9] and [17].

Measured results were then compared to numerical predictions considering the digital twin model. The measured and simulated nominal-to-peak amplitude and phase variation within the QZ volume are shown in Fig. 6 and Fig. 7 respectively, for both polarization of the PWG.

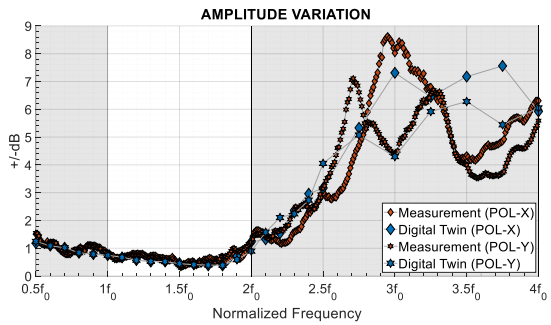

Fig. 6. Measured and simulated (digital-twin) worst case, nominal-to-peak amplitude variations over the QZ volume with dedicated wide-band optimisation in the f_0 to $2f_0$ frequency range for the 19-element array.

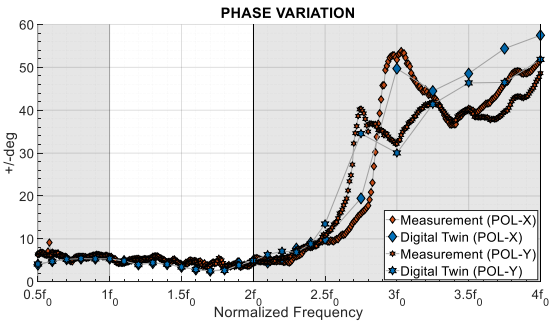

Fig. 7. Measured and simulated (digital-twin) worst case, nominal-to-peak phase variations over the QZ volume with dedicated wide-band optimisation in the f_0 to $2f_0$ frequency range for the 19-element array.

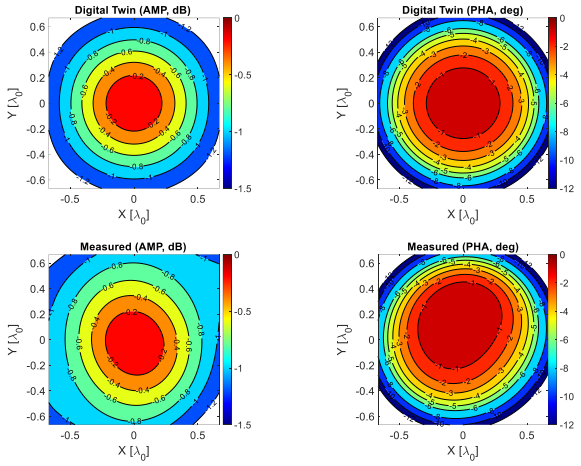

Fig. 8. Measured and simulated (digital-twin) amplitude and phase variations over the center QZ cross range at the center $1.5f_0$ frequency for the 19-element array using wide-band coefficients optimized at f_0 to $2f_0$.

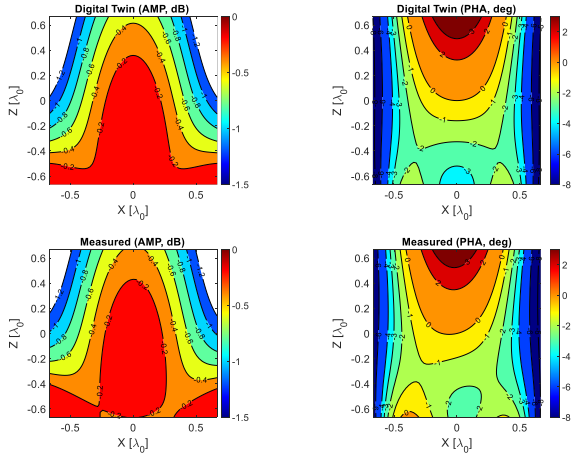

Fig. 9. Measured and simulated (digital-twin) amplitude and phase variations over the QZ down range at the center $1.5f_0$ frequency for the 19-element array using wide-band coefficients optimized at f_0 to $2f_0$.

A comparison of the measured and predicted (digital twin) amplitude and phase variation within the QZ cross-range and down-range at $1.5fo$ frequency are shown in Fig. 8 and Fig. 9, respectively. Minimal differences between measurements and predictions are observed, indicating that the PWG concept can be easily scaled to other frequency bands.

Comparisons between digital twin and measured PWG in terms of NF directivity patterns [17] are shown in Fig. 10 at fo and $1.5fo$. The patterns are evaluated on a sphere of radius $R = 3\lambda o$ intersecting QZ center. In addition to the strong agreement between the digital twin and measured data, this analysis demonstrates that most of the energy is concentrated within the QZ region (with a field of view of approximately $\theta = \pm 10°$), while illumination, and therefore energy, outside this region is significantly reduced, as expected from the optimized PWG excitation. This feature is crucial for the PWG, enabling highly efficient anechoic performance even within a reduced volume, compared to other solutions.

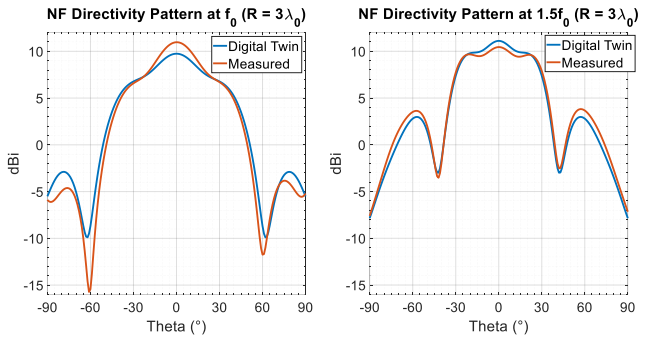

Fig. 10. NF directivity patterns evaluated on the sphere intersecting the QZ center ($R = 3\lambda_0$). Comparison between digital twin and measured PWG at f_0 and $1.5f_0$ (E-plane cut of the X-polarization of the PWG).

The NF gain [17] over frequency, evaluated at the center of the QZ is shown Fig. 11. Once again, the comparison between predictions and measurement is excellent for both polarizations of the PWG. Comparing the NF gain and the NF directivity, the losses (i.e. efficiency) of the PWG are derived and range from -18dB and -24dB in the optimized sub-band f_0 to $2f_0$. The insertion loss of the BFN components such as phase shifters and power dividers significantly contribute to such relatively high loss of the system. As shown [15], this can be optimized considering the tradeoff between QZ uniformity and power density in the QZ.

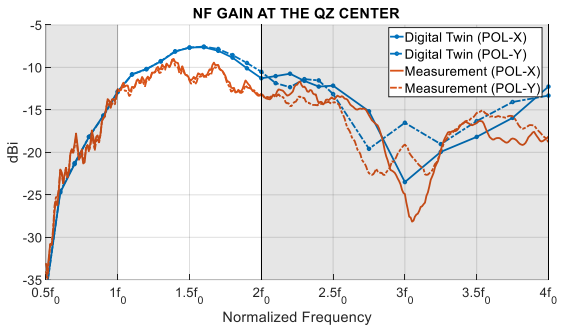

Fig. 11. NF gain evaluted at the center of the QZ. Comparison between digital twin and measured PWG.

VI. Conclusion

A PWG solution for VHF/UHF frequency measurements with dual polarization and an intended 10:1 operating frequency bandwidth has been presented. The beamforming network is designed to maintain constant excitation coefficients across the entire bandwidth, making it ideal for time-domain testing, as well as testing wideband antennas and devices with modulated signals.

The use of fixed excitation across wider bandwidths was investigated through a dedicated optimization of the array's complex weights, resulting in a novel optimization strategy. This concept was validated through both simulations and measurements on a 19-element array. Measurements were performed over a 8:1 bandwidth, covering the frequency range from $\boldsymbol{0.5f_0}$ to $\boldsymbol{4f_0}$, where $\boldsymbol{f_0}$ represents the lowest design frequency. Both simulations and measurements demonstrated excellent QZ performance across and beyond the target bandwidth, confirming the effectiveness of the wideband array excitation optimization.

Acknowledgment

The authors would like to thank the Pulsaart team, represented by Yvain Cornet, Arthur Romeijer and Vincent Vandenberghe, for their hospitality and continuous support during the measurement campaign.

References

[1] IEEE Std 149-2021 “IEEE Recommended Practice for Antenna Measurements”

[2] IEEE Std 1720-2012 “Recommended Practice for Near-Field Antenna Measurements”

[3] Z. Yang, Z. Wang, Y. Zhang and S. Gao, "Robust Plane Wave Generator Design in Small Anechoic Chamber Setup Using Parameterized Field Method," in *IEEE Access*, vol. 8, pp. 187052-187059, 2020

[4] Y. Zhang, Z. Wang, X. Sun, Z. Qiao, W. Fan and J. Miao, "Design and implementation of a wideband dual-polarized plane wave generator with tapered feeding nonuniform array", *IEEE Antennas Wireless Propag. Lett.*, vol. 19, no. 11, pp. 1988-1992, Nov. 2020

[5] O. M. Bucci, M. D. Migliore, G. Panariello and D. Pinchera, "Plane-wave generators: Design guidelines achievable performances and effective synthesis", *IEEE Trans. Antennas Propag.*, vol. 61, no. 4, pp. 2005-2018, Apr. 2013

[6] A. Capozzoli, C. Curcio, G. D'Elia, A. Liseno and P. Vinetti, "A novel approach to the design of generalized plane-wave synthesizers," *2009 3rd European Conference on Antennas and Propagation*, Berlin, Germany, 2009, pp. 3375-3379

[7] R. Haupt, "Synthesis of a plane wave in the near field with a planar phased array", *IEEE Antennas and Propagation Society International Symposium*, pp. 792-795, 2003.

[8] Daniele Pinchera, Marco Donald Migliore, "Efficient Synthesis of Concentric-Rings Plane Wave Generators", *IEEE Transactions on Antennas and Propagation*, vol.71, no.6, pp.4967-4975, 2023

[9] F. Scattone *et al.*, "Design of Dual Polarised Wide Band Plane Wave Generator for Direct Far-Field Testing," *2019 13th European Conference on Antennas and Propagation (EuCAP)*, Krakow, Poland, 2019

[10] C. Rowell and A. Tankielun, "Plane wave converter for 5G massive MIMO Basestation measurements", *Proc. 12th Eur. Conf. Antennas Propag.*, pp. 1-3, 2018

[11] F. Scattone et al. “Preliminary Assesment of Millimeter Wave Plane Wave Generator For 5G Device Testing”EuCAP 2021, 22-26 March 2021, Düsseldorf, Germany

[12] F. Saccardi et al. "Uncertainty of a VHF CubeSat Measurement based on the Synthetic Probe Array Technique,“ EuCAP2023

[13] V. Schirosi F. Saccardi, A. Giacomini, F. Scattone, L. Scialacqua, A. Diamanti, E. Tartaglino, L.J. Foged, N. Gross, S. Anwar, E. Kaverine, P.O. Iversen, E. Szpindor, “Accurate Antenna Characterisation at VHF/UHF Frequencies with Plane Wave Generator Systems” AMTA2023

[14] F. Scattone *et al.*, “Plane Wave Generator for Direct Far-field Over-The-Air Testing of Devices”, Symposium of the Antenna Measurement Techniques Association, AMTA, Williamsburg, USA, 2018.

[15] P. E. Frandsen and S. B. Sørensen, "Formulations of the contoured beam array antenna minmax optimization problem", Proceedings of the 1994 Progress in Electromagnetics Research Symposium, European Space Agency, Noordwijk, The Netherlands, Jul. 1994

[16] https://www.pulsaart.com/

[17] F. Saccardi, A. Giacomini, L. J. Foged “Accurate Evaluation of Antenna Measurement Range Performance with the SWE Transmission Formula” AMTA 2023, October 8-13, Seattle, WA, USA